

# Day-Ahead Electricity Price Forecasting Using a Multivariate Group Lasso Method

Keyi Wang<sup>a</sup>, Jiaxiang Ji<sup>a</sup>, Mahan Mansouri<sup>b</sup> and Ahmed Aziz Ezzat<sup>a,\*</sup>

<sup>a</sup>Rutgers, The State University of New Jersey, Piscataway, 08854, New Jersey, United States of America

<sup>b</sup>PG&E, Pacific Gas & Electric Company, Oakland, 94612, California, United States of America

---

## ARTICLE INFO

*Keywords:*  
Forecasting  
Electricity Prices  
Electricity Markets  
Group Lasso

## ABSTRACT

Electricity price signals in modern power systems exhibit complex dependence structures that render forecasting inherently challenging. Our analysis of real-world pricing signals from the California Independent System Operator (CAISO) reveals complex temporal group effects, whereby the influence of explanatory variables on electricity prices persists across consecutive blocks of time due to underlying economic and operational drivers. In response, we propose a multivariate statistical method based on a Group Lasso formulation to forecast the vector of day-ahead electricity prices, by leveraging multi-feature temporal group effects. Our approach is evaluated on two full years of electricity prices from CAISO, demonstrating considerable improvements in point and probabilistic forecast metrics compared to a wide array of statistical and deep learning methods. Theoretical and empirical analyses confirm the effectiveness of the proposed approach in modeling realistic group effects, maintaining both interpretability and low computational complexity. When retrospectively evaluated on test data from a recent international electricity price forecasting challenge, the proposed method ranked in second place, despite having access to significantly less information than competing approaches. Finally, the proposed method is independently validated against two operational electricity price forecasting systems in CAISO, demonstrating competitive predictive performance and practical relevance.

---

## 1. Introduction

In modern power systems, accurate short-term electricity price forecasts are critical for reliable and economically efficient decision-making by system operators and electricity market participants. For system operators, accurate day-ahead forecasts of pricing signals support secure system balancing and market clearing, while for power producers, they inform bidding strategies, production scheduling, and asset management across electricity market operations [1–3]. Given the substantial economic consequences associated with forecast errors, effective short-term electricity price forecasting (EPF) has become an essential component of modern power system operations and market participation.

Over the past two decades, numerous approaches have been proposed for short-term EPF, spanning both statistical and machine learning (ML) paradigms [4, 5]. The vast majority of statistical methods for EPF are rooted in time-series and regression models which explicitly encode autocorrelations, seasonal patterns, and dynamic covariate effects. Representative examples include dynamic regression and autoregressive-based models [6, 7], exponential smoothing approaches [8], and regime-switching models for handling non-linear structural changes [9]. Multivariate methods and regularized models have also shown significant promise in short-term EPF, especially when a large set of exogenous features is invoked. These include those based on Lasso, Elastic Net, and related variants [10–12]. More recently, ML-based approaches have gained substantial attention due to their ability to learn complex drivers of pricing signals from large feature sets. This line of work includes tree-based and ensemble learning models [13, 14], kernel-based approaches [15], as well as deep neural networks (DNNs), including those based on recurrent [16], convolutional [17], autoencoder-based and generative models [18, 19], as well as transformer-based architectures [20].

There are pros and cons for the statistical and ML approaches for short-term EPF. Overall, statistical methods remain prevalent in practice because they are relatively simpler to train, easier to interpret, and have demonstrated competitive predictive performance especially for shorter forecast horizons. Among these statistical approaches, we would like to especially shed light on the Lasso-estimated autoregressive (LEAR) model, which is a well-established and well-proven statistical method for short-term EPF [10]. LEAR is a parameter-rich linear regression model for day-ahead EPF which leverages Lasso regularization to account for diverse covariate sets efficiently, including historical

---

\*Corresponding author

✉ [aziz.ezzat@rutgers.edu](mailto:aziz.ezzat@rutgers.edu) (A.A. Ezzat)

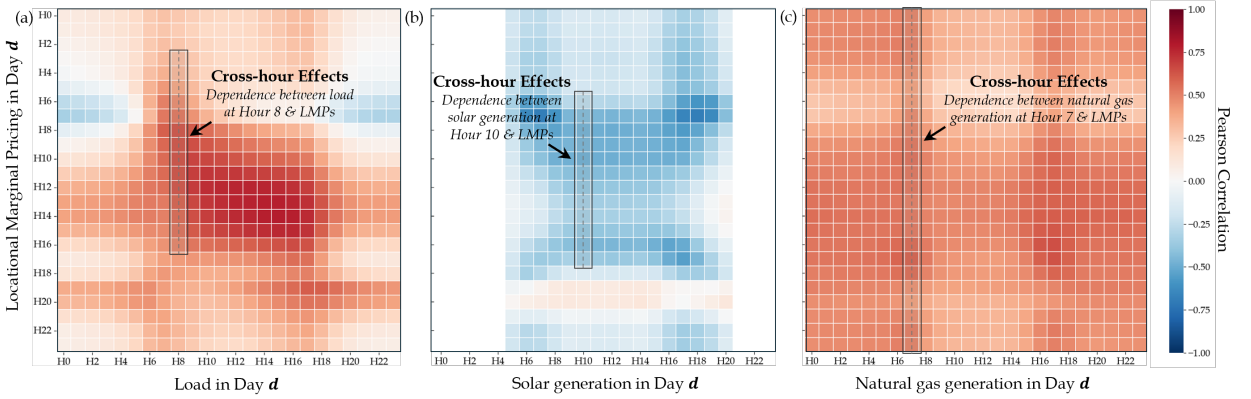


**Figure 1:** Pearson correlation heatmaps between LMPs and forecasts of regional load (a), solar generation (b), and natural gas generation (c), respectively, during 2025 in CAISO. The plots reveal strong cross-hour (non-local) temporal dependencies between key system variables and LMPs, wherein each column shows the dependence between a single-hour variable (e.g., regional load at hour 8) and the correspondent intra-day LMPs. The structured, non-local patterns highlight the importance of modeling temporal group effects in LMPs, which is not captured by hour-wise independent models.

price patterns, operational, economic, environmental, and calendar effects. Recent large-scale experiments suggest that LEAR’s performance is on par with, if not better than, that of DNNs, with the added advantages of providing interpretable covariate effect explanations (in the form of estimated coefficients), and having compute costs that are substantially smaller for both model training and evaluation, favoring their adoption for operational forecasting applications in electricity systems [21].

Despite these favorable properties, a key limitation of the LEAR model lies in its treatment of temporal dependence. In its standard formulation, LEAR models each hourly price independently. Treating each hour as a separate learning task can overlook systematic similarities in how explanatory variables, such as load and generation, influence prices over time. There is an active line of research to effectively model cross-hour dependencies by adopting fully multivariate formulations, where the hourly day-ahead prices are modeled jointly rather than as independent outputs. A common approach in this context is vector autoregression (VAR) [22–24]. However, VAR models can become challenging to scale with increasing dimensionality, particularly in the presence of large feature sets. There are dimension-reduction strategies such as factor-based and reduced-rank structures that have been proposed to capture cross-hour dependence with a smaller set of parameters [25–27]. Another alternative for multivariate modeling is to design a multi-output DNN architecture with a vectorized output representing the hourly day-ahead prices [11, 21].

While the above approaches can model cross-hour dependencies, they do not explicitly enforce a key practical requirement: consistent predictor selection over time. This is especially relevant in the presence of *temporal group effects*, whereby the explanatory features influence prices over contiguous blocks of time periods rather than at isolated time points, reflecting underlying operational and economic dynamics. These cross-hour group effects arise from the temporal coupling inherent in electricity system operations. For example, load and generation at a given hour affect unit commitment, ramping decisions, and reserve requirements across multiple hours, leading to non-local dependencies in electricity prices. Price formation is therefore naturally governed by inter-temporal operational constraints that induce structured dependencies across consecutive blocks of time periods.

Our analysis of actual pricing signals from the California Independent System Operator (CAISO) further supports this observation. Figure 1 shows the strength of Pearson correlations (evaluated using a full year of data from CAISO) between the hourly locational marginal prices (LMP) and the correspondent forecasts of exogenous features, namely system load (Panel a), solar generation (Panel b), and natural gas generation (Panel c). In the absence of cross-hour dependence, one would expect the influence of an hourly explanatory variable (load, solar, or natural gas generation) to be primarily localized to the corresponding hourly LMP, resulting in a correlation structure concentrated along the diagonal of the heatmaps shown in Figure 1. Instead, the correlation heatmaps exhibit clear vertical band structures, suggesting that a given hourly feature is strongly correlated with LMPs across several consecutive hourly blocks. For example, morning load levels in Figure 1(a) (hours 6–12) display strong and temporally persistent correlations with LMPs throughout the day. Similarly, daytime solar generation in Figure 1(b) (hours 6–19) shows consistent

negative correlations across most time periods, whereas natural gas generation in Figure 1(c) exhibits consistent positive correlations with LMPs across almost all hours, with relatively stronger effects during sunrise and sunset periods (hours 6–8 and 16–17).

To model these cross-hour group effects, we propose a multivariate statistical model for short-term EPF, which we dub as the “Cross-Influence-Group-Lasso-Estimated Auto-Regressive” model, or in short CING-LEAR (pronounced as Shakespeare’s *King Lear*). CING-LEAR generalizes the LEAR model to a multivariate setting through a group regularization. Our primary contributions are summarized as follows:

- We propose a multivariate EPF model which accounts for cross-hour feature group effects that are prevalent in electricity pricing signals. CING-LEAR extends the LEAR framework to a multi-output setting and is formulated with a Group Lasso regularizer, enabling the joint selection of covariate effects across the full forecast horizon. We posit that this group-wise sparsity structure is more naturally aligned with the inter-temporal dependencies induced by electricity system operations.
- We extensively evaluate CING-LEAR on two years of LMPs from CAISO. Theoretical and empirical analyses confirm its effectiveness in capturing realistic group effects. Forecasting results suggest considerable improvements in both point and probabilistic forecast metrics (14% and 13% reduction in RMSE and CRPS, respectively). When retrospectively evaluated on a recent international electricity price forecasting challenge, CING-LEAR ranked in second place, despite having access to significantly less information than competing approaches. Finally, the method is independently benchmarked against two operational forecasting systems currently deployed by a major U.S. utility where it demonstrates competitive performance and practical relevance.

The remainder of this paper is organized as follows. Section 2 describes the data used in this work. Section 3 details the formulation of CING-LEAR. Section 4 introduces the experimental setup and evaluation metrics, followed by Section 5 where the results are presented. Finally, Section 6 concludes the paper and highlights future research directions.

## 2. Data description

Four years of day-ahead LMPs, along with exogenous information about load, generation, and fuel prices, are extracted from the Gridstatus API [28] for the CAISO NP15 region, spanning from January 2022 to December 2025 at hourly resolution. Solar generation is directly available at the NP15 region, whereas other exogenous variables are available at different spatial resolutions. Specifically, load data are obtained from the PG&E TAC area which closely corresponds to the geographic scope of the NP15 region. Natural gas generation is available only at the system level, while fuel prices are sourced from the BANC region.

Figure 2 illustrates the forecasting setup. Standing at day  $d$ , we forecast the hourly LMPs of day  $d + 1$  before the day-ahead market closure time (10:00am). To do so, the model is trained using data from the previous three years, including the  $d$ th day prices since the CAISO day-ahead market results are published at 1:00pm on the day prior to the trade day. For all exogenous covariates, we use forecasts provided by CAISO when available; otherwise, forecasts are generated using in-house models. CAISO publishes their day-ahead forecasts for load and solar generation prior to market closure, released at 9:00am and 8:45am, respectively. In contrast, forecasts for natural gas generation and fuel prices are not publicly available, so we generate these forecasts internally, as described next.

For natural gas generation, we use an ARIMA-X model. Letting  $g_{d,h}$  denote the natural gas generation at hour  $h$  on day  $d$ , then, its forecast model is specified as in (1).

$$\hat{g}_{d,h}^{\text{ARIMA-X}} = \phi_0 + \sum_{i=1}^p \phi_i g_{d,h-i} + \sum_{j=1}^q \theta_j \varepsilon_{d,h-j} + \beta_1 g_{d-7,h} + \beta_2 \hat{\ell}_{d,h} + \beta_3 \hat{s}_{d,h} + \varepsilon_{d,h}, \quad \forall h \in \{1, \dots, 24\}, \quad (1)$$

where  $\{\phi_i\}$  and  $\{\theta_j\}$  denote auto-regressive and moving-average coefficients, respectively. In (1),  $g_{d-7,h}$  denotes the natural gas generation at the same hour one week earlier, whereas  $\hat{\ell}_{d,h}$  and  $\hat{s}_{d,h}$  are the load and solar forecasts issued by CAISO, respectively, and  $\varepsilon_{d,h}$  is a stochastic error term. We experiment with various model configurations and training periods, and conclude that a model order of  $p = q = 1$ , with a training length of 7 days yields a sufficiently accurate performance. Fuel prices, on the other hand, are constant within each day, and are known at the time of forecasting for the  $d$ th day. We therefore adopt a persistence forecast to predict day-ahead fuel prices.

## Day-Ahead Electricity Price Forecasting

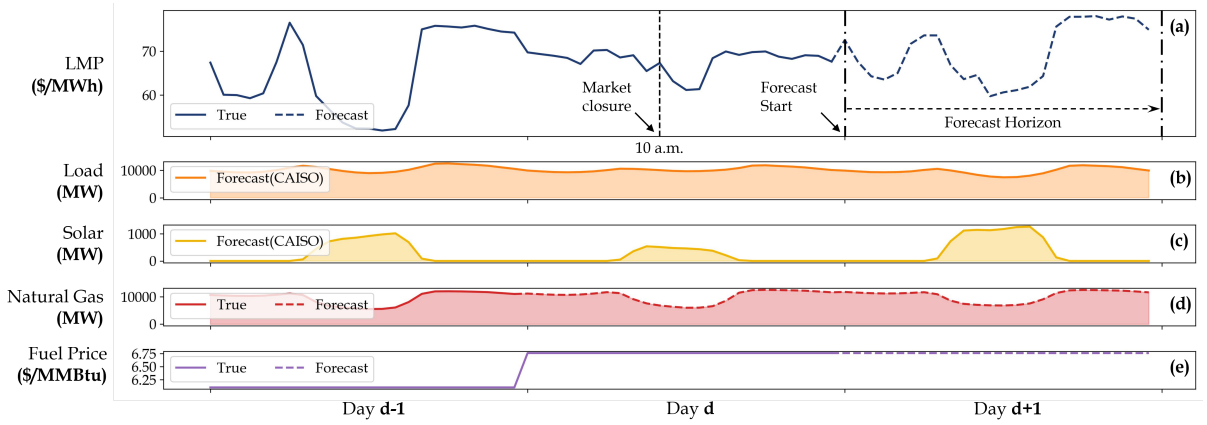


**Figure 2:** Time series illustration of LMPs and exogenous variables over a three-day horizon. The vertical dashed line in panel (a) denotes the day-ahead market closure time (10:00am), at which the LMP for day  $d + 1$  is forecasted. Across all panels, solid lines indicate information that are available before the market closure time, while dashed lines represent information that are not available and therefore must be forecasted. Specifically, in panels (a), (d), and (e), solid lines correspond to true values and dashed lines denote forecasted values. Panels (b) and (c) display forecasted values only, as provided by CAISO.

Overall, LMPs exhibit a strong positive correlation with fuel prices (0.74 on a Pearson correlation scale), and a moderate positive correlation with regional load (0.36 on a Pearson correlation scale), while showing a moderate to weak negative correlation with solar generation ( $-0.26$  on a Pearson correlation scale). Natural gas generation, which often serves as a complementary resource to variable solar generation as illustrated in Figure 2 (c)-(d), is also positively correlated with LMP (0.44 on a Pearson correlation scale).

### 3. Methodology

We begin by formally defining important notation in Section 3.1, followed by a brief overview of the LEAR method in Section 3.2. From there, we introduce the building blocks of the proposed approach, CING-LEAR, in Section 3.3.

#### 3.1. Model inputs and notation

Let  $p_{d,h}$  denote the day-ahead electricity price for day  $d$  and hour  $h \in \{1, \dots, 24\}$ . We collect the hourly prices for day  $d$  in the vector,  $\mathbf{p}_d$  defined as follows:

$$\mathbf{p}_d = (p_{d,1}, \dots, p_{d,24})^\top \in \mathbb{R}^{24}.$$

For the exogenous variables, we use the day-ahead forecasts of  $K$  variables. For each variable  $k \in \{1, \dots, K\}$  we denote the hourly forecast for day  $d$  by:

$$\mathbf{x}_d^{(k)} = (x_{d,1}^{(k)}, \dots, x_{d,24}^{(k)})^\top \in \mathbb{R}^{24}.$$

The input features used to predict the 24-dimensional price vector  $\mathbf{p}_d$  for day  $d$  include the following:

- Historical day-ahead prices of the previous three and seven days, respectively:

$$\mathbf{p}_{d-1}, \mathbf{p}_{d-2}, \mathbf{p}_{d-3}, \mathbf{p}_{d-7}.$$

- Day-ahead forecasts of the  $K$  exogenous variables for days  $d$ ,  $d - 1$  and  $d - 7$ :

$$\{\mathbf{x}_d^{(k)}, \mathbf{x}_{d-1}^{(k)}, \mathbf{x}_{d-7}^{(k)} : k = 1, \dots, K\}.$$

- A vector of dummy variables denoting the day-of-week variation:

$$\mathbf{z}_d = (z_{d,1}, \dots, z_{d,7})^\top \in \{0, 1\}^7,$$

where  $z_{d,j} = 1$  if day  $d$  is the  $j$ -th day of the week and  $z_{d,j} = 0$  otherwise.

For notational convenience, we stack all features available on day  $d - 1$  for predicting  $\mathbf{p}_d$  into a single vector:

$$\mathbf{x}_d = [\mathbf{p}_{d-1}^\top, \mathbf{p}_{d-2}^\top, \mathbf{p}_{d-3}^\top, \mathbf{p}_{d-7}^\top, \{\mathbf{x}_d^{(k)\top}\}_{k=1}^K, \{\mathbf{x}_{d-1}^{(k)\top}\}_{k=1}^K, \{\mathbf{x}_{d-7}^{(k)\top}\}_{k=1}^K, \mathbf{z}_d^\top]^\top \in \mathbb{R}^M,$$

such that  $M$  denotes the total number of input regressors. Given a dataset of  $N$  days  $\{d = 1, \dots, N\}$ , we define the design (or regression) matrix as follows:

$$\mathbf{X} = \begin{bmatrix} \mathbf{x}_1^\top \\ \vdots \\ \mathbf{x}_N^\top \end{bmatrix} \in \mathbb{R}^{N \times M}.$$

### 3.2. Background on the LEAR model for short-term EPF

Here, we briefly review LEAR, a well-established statistical model for short-term EPF [10]. LEAR models the electricity price  $p_{d,h}$  on day  $d$  and hour  $h$  using a parameter-rich linear regression formulation as in (2).

$$p_{d,h} = \mathbf{x}_d^\top \boldsymbol{\beta}_h + \varepsilon_{d,h}, \quad d = 1, \dots, N, \quad h = 1, \dots, 24, \quad (2)$$

where  $\boldsymbol{\beta}_h \in \mathbb{R}^M$  denotes an hour-specific vector of regression coefficients, and  $\varepsilon_{d,h}$  denotes a zero-mean error term.

LEAR estimates each parameter set  $\boldsymbol{\beta}_h$  independently using a Lasso regularization method, which imposes an  $\ell_1$  penalty on the coefficient vector in order to perform automatic and sparse feature selection. Specifically, for each hour  $h \in \{1, \dots, 24\}$ , the parameter set  $\boldsymbol{\beta}_h$  is estimated using the expression in (3).

$$\hat{\boldsymbol{\beta}}_h = \arg \min_{\boldsymbol{\beta} \in \mathbb{R}^M} \left\{ \frac{1}{N} \sum_{d=1}^N (p_{d,h} - \mathbf{x}_d^\top \boldsymbol{\beta})^2 + \lambda_h \|\boldsymbol{\beta}\|_1 \right\}, \quad (3)$$

This hour-by-hour Lasso strategy produces an independent coefficient vector  $\hat{\boldsymbol{\beta}}_h$  for each hour  $h$ , enabling the set of selected predictors to vary across the forecast horizon.

### 3.3. The proposed CING-LEAR model for short-term EPF

The motivation for CING-LEAR follows directly from the cross-hour feature group effects observed in CAISO's pricing signals—recall Figure 1. The observations made therein motivate us to formulate a multivariate extension of LEAR which specifically incentivizes consistent feature selection across consecutive blocks of time periods, rather than estimating each localized hourly effect independently.

The conceptual difference between LEAR and CING-LEAR can be understood through the coefficient organization scheme shown in Figure 3. LEAR estimates 24 hour-specific coefficient vectors  $\{\boldsymbol{\beta}_h\}_{h=1}^{24}$  and applies an  $\ell_1$  penalty to each  $\boldsymbol{\beta}_h$  independently. This hour-by-hour strategy allows different subsets of predictors to be selected for different hours, which can be flexible but does not explicitly encode the cross-hour dependence implied by Figure 1. In contrast, CING-LEAR organizes the coefficients so that each predictor forms a single group across the 24 hourly outputs. This design directly mirrors the vertical-band structure shown in Figure 1: if a covariate tends to consistently influence the electricity prices across hourly blocks, it is natural to treat its day-ahead hourly coefficients as one structured object and then regularize it jointly. As such, a covariate is selected consistently across the full day-ahead horizon, enabling the model to capture cross-hour feature group effects while maintaining model sparsity.

Specifically, we collect the hourly coefficients into a single coefficient matrix,  $\mathbf{B}$ , defined as:

$$\mathbf{B} = [\boldsymbol{\beta}_1, \dots, \boldsymbol{\beta}_{24}] \in \mathbb{R}^{M \times 24},$$

where the  $h$ -th column  $\boldsymbol{\beta}_h$  contains the regression coefficients for hour  $h$ . For each day  $d$ , the multivariate linear regression model adopted in CING-LEAR is expressed as in (4).

$$\mathbf{p}_d = \mathbf{B}^\top \mathbf{x}_d + \varepsilon_d, \quad d = 1, \dots, N, \quad (4)$$

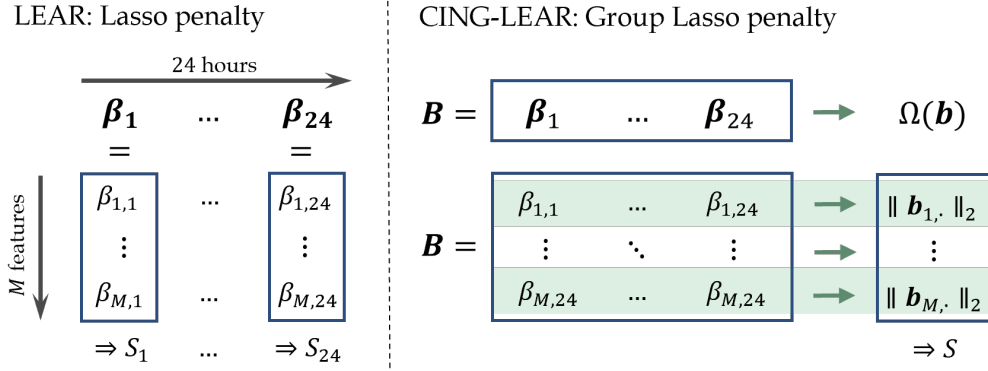


**Figure 3:** Conceptual difference between the regularization structure in LEAR (left) versus its proposed multivariate extension, CING-LEAR (right).

where  $\boldsymbol{\varepsilon}_d \in \mathbb{R}^{24}$  collects the hourly errors. Stacking all days, we collect the pricing vectors and error terms in the matrices  $\mathbf{P}$  and  $\mathbf{E}$ , respectively, defined as:

$$\mathbf{P} = \begin{bmatrix} \mathbf{p}_1^\top \\ \vdots \\ \mathbf{p}_N^\top \end{bmatrix} \in \mathbb{R}^{N \times 24}, \quad \mathbf{E} = \begin{bmatrix} \boldsymbol{\varepsilon}_1^\top \\ \vdots \\ \boldsymbol{\varepsilon}_N^\top \end{bmatrix} \in \mathbb{R}^{N \times 24}.$$

Then, the formulation in (4) can be written in matrix format as in (5).

$$\mathbf{P} = \mathbf{X}\mathbf{B} + \mathbf{E}. \quad (5)$$

Let  $\mathbf{b}_{j,\cdot}^\top$  denote the  $j$ -th row of  $\mathbf{B}$ , corresponding to the coefficients of feature  $j$  across all 24 hours:

$$\mathbf{b}_{j,\cdot} = (\beta_{j,1}, \dots, \beta_{j,24})^\top \in \mathbb{R}^{24}, \quad j = 1, \dots, M.$$

To enforce joint feature selection across hours, we apply a group Lasso penalty on the rows of  $\mathbf{B}$ . Specifically, the penalty is defined as:

$$\Omega(\mathbf{B}) = \sum_{j=1}^M \|\mathbf{b}_{j,\cdot}\|_2,$$

which encourages entire rows of  $\mathbf{B}$  to shrink to zero. As a consequence, feature  $j$  is either selected for all hours or removed simultaneously from the model.

Given  $\mathbf{X}$  and  $\mathbf{P}$ , CING-LEAR solves the optimization problem expressed in (6).

$$\hat{\mathbf{B}} = \arg \min_{\mathbf{B} \in \mathbb{R}^{M \times 24}} \left\{ \frac{1}{N} \|\mathbf{P} - \mathbf{X}\mathbf{B}\|_F^2 + \lambda \Omega(\mathbf{B}) \right\}, \quad (6)$$

where  $\|\cdot\|_F$  denotes the Frobenius norm and  $\lambda \geq 0$  is a regularization hyperparameter controlling the degree of sparsity.

Compared with LEAR, our formulation jointly estimates the full coefficient matrix  $\mathbf{B}$ , which results in a comparatively large set of parameters. In this case, the group Lasso enforces sparsity enabling consistent feature selection by exploiting the cross-hour group structure in electricity pricing signals.

Given the fitted coefficient matrix  $\hat{\mathbf{B}}$  obtained from (6), the day-ahead point forecast of price vector  $\mathbf{p}_d \in \mathbb{R}^{24}$  can be defined as in (7).

$$\hat{\mathbf{p}}_d = \mathbb{E}(\mathbf{p}_d | \mathbf{x}_d) = \hat{\mathbf{B}}^\top \mathbf{x}_d. \quad (7)$$

---

**Algorithm 1** Sliding Window Implementation of CING-LEAR
 

---

- 1: **Parameters:** calibration window length  $N$ , test length  $L$   
     CV folds  $K$ , regularization size  $n_\lambda$ , maximum iterations  $I_{\max}$
  - 2: Initialize iteration counter  $\ell = 1$
  - 3: **while**  $\ell \leq L$  **do**
  - 4:     Input data of previous  $N$  days before day  $\ell$
  - 5:     Build training data:  $\mathbf{X} \leftarrow \{x_{d,h}\}_{d=1,\dots,N, h=1,\dots,24}$ ,  $\mathbf{P} \leftarrow \{p_{d,h}\}_{d=1,\dots,N, h=1,\dots,24}$
  - 6:     Build forecast data:  $\mathbf{X}_\ell \leftarrow \{x_{d,h}\}_{d=1,\dots,N+1, h=1,\dots,24}$
  - 7:     Select regularization  $\lambda_\ell^*$  via  $CV(K, n_\lambda, I_{\max})$
  - 8:      $\widehat{\mathbf{B}}_\ell \leftarrow \text{CING-LEAR}(\mathbf{X}, \mathbf{P}; \lambda_\ell^*, I_{\max})$
  - 9:     Generate day-ahead 24-hour forecast:  $\widehat{\mathbf{P}}_\ell \leftarrow \mathbf{X}_\ell \widehat{\mathbf{B}}_\ell$
  - 10:     $\ell \leftarrow \ell + 1$
  - 11: **end while**
  - 12: **return**  $\widehat{\mathbf{B}} = \{\widehat{\mathbf{B}}_1, \dots, \widehat{\mathbf{B}}_L\}$ ,  $\widehat{\mathbf{P}} = \{\widehat{\mathbf{P}}_1, \dots, \widehat{\mathbf{P}}_L\}$
- 

Uncertainty information can be derived by imposing a distributional assumption on the error vector. Specifically, we let  $\epsilon_d \sim \mathcal{N}(\mathbf{0}, \mathbf{\Sigma})$ , such that  $\mathbf{\Sigma} \in \mathbb{R}^{24 \times 24}$  is a symmetric positive definite matrix that captures the dependence structure of forecast errors across different hours. Under this assumption, the conditional distribution of the day-ahead price vector given the feature vector  $\mathbf{x}_d$  can be expressed as in (8).

$$\mathbf{p}_d \mid \mathbf{x}_d \sim \mathcal{N}(\widehat{\mathbf{B}}^\top \mathbf{x}_d, \mathbf{\Sigma}). \quad (8)$$

The covariance matrix  $\mathbf{\Sigma}$  can be estimated from in-sample residuals using the empirical covariance estimator, as in (9).

$$\widehat{\mathbf{\Sigma}} = \frac{1}{N} \sum_{d=1}^N \widehat{\epsilon}_d \widehat{\epsilon}_d^\top, \quad (9)$$

such that  $\widehat{\epsilon}_d = \mathbf{p}_d - \widehat{\mathbf{B}}^\top \mathbf{x}_d$ . The resulting predictive distribution enables the construction of useful uncertainty outputs, including prediction intervals and scenario generation, while explicitly accounting for cross-hour error dependence.

For training and evaluation, we adopt a sliding window approach spanning two full years from 2024 to 2025. Since the full dataset starts in 2022, all tests in 2024 are calibrated using data from January 2022 up to the forecast date; whereas for tests in 2025, calibration is performed using data from the three years prior to each forecast date. Algorithm 1 shows the steps of this sliding window approach. On each testing day, the optimal regularization parameter  $\lambda^*$  is selected via five-fold cross-validation over  $n_\lambda = 100$  candidate values, with a maximum of  $I_{\max} = 5000$  iterations. The coefficient matrix  $\widehat{\mathbf{B}}$  is then estimated by solving the optimization problem in (6) using a coordinate descent algorithm [29], which alternates between updating groups of coefficients while keeping the remaining parameters fixed. This approach is computationally efficient and particularly effective for sparse, multi-task regression problems [30]. With the estimated coefficient matrix, the day-ahead forecast can be generated. Finally, all estimated coefficient matrices and the corresponding forecasts over the entire testing period are saved for reporting.

## 4. Experimental Setup

In this section, we describe data preprocessing steps, benchmarks, and metrics used to evaluate CING-LEAR.

### 4.1. Data Preprocessing

To improve the numerical stability of the model, we preprocess electricity prices in two steps, a normalization and a transformation, as recommended in [21, 31].

Let  $p_{d,h}$  denote the price at day  $d$  and hour  $h$ . The normalized price is defined as:

$$\tilde{p}_{d,h} = \frac{p_{d,h} - a}{b}, \quad (10)$$

where  $a$  is the median of the in-sample prices, and  $b$  is the sample median absolute deviation (MAD) adjusted by a factor  $1.4826 \approx 1/z_{0.75}$  where  $z_{0.75}$  is the 75th percentile of the standard normal distribution. After normalization, we apply the inverse hyperbolic sine transformation. The transformed price is given by:

$$\text{asinh}(\tilde{p}_{d,h}) = \log \left( \tilde{p}_{d,h} + \sqrt{\tilde{p}_{d,h}^2 + 1} \right). \quad (11)$$

## 4.2. Benchmarks

Several representative benchmarks in EPF studies are considered. All benchmark models are implemented under the same sliding window setup as in CING-LEAR.

### 4.2.1. Naïve

The Naïve approach is a standard benchmark in the forecasting literature and practice and simply assumes persistence of LMPs, as in (12).

$$\hat{p}_{d,h}^{\text{Naïve}} = p_{d-1,24}, \quad \forall h \in \{1, \dots, 24\}. \quad (12)$$

### 4.2.2. Seasonal Naïve

The Seasonal Naïve extends the naïve model by accounting for daily seasonality, as in (13).

$$\hat{p}_{d,h}^{\text{S-Naïve}} = p_{d-1,h}, \quad \forall h \in \{1, \dots, 24\}. \quad (13)$$

### 4.2.3. ARIMA

The autoregressive integrated moving average (ARIMA) model is a univariate time series approach which linearly extrapolates historical signals, as in (14).

$$\hat{p}_{d,h}^{\text{ARIMA}} = \phi_0 + \sum_{i=1}^p \phi_i p_{d,h-i} + \sum_{j=1}^q \theta_j \varepsilon_{d,h-j} + \varepsilon_{d,h}, \quad \forall h \in \{1, \dots, 24\}. \quad (14)$$

### 4.2.4. ARIMA-X

The ARIMA-X includes exogenous variables in the ARIMA structure, as in (15).

$$\hat{p}_{d,h}^{\text{ARIMA-X}} = \phi_0 + \sum_{i=1}^p \phi_i p_{d,h-i} + \sum_{j=1}^q \theta_j \varepsilon_{d,h-j} + \sum_{k=1}^K \beta_k x_{d,h}^{(k)} + \varepsilon_{d,h}, \quad \forall h \in \{1, \dots, 24\}, \quad (15)$$

where  $x_{d,h}^{(k)}$  represents the day-ahead forecast of the  $k$ -th exogenous variable. For fair comparison, same exogenous information as CING-LEAR are considered, including forecasts of regional load, solar generation, natural gas generation, and fuel prices, together with the day-of-week indicators.

### 4.2.5. LEAR

The Lasso-Estimated Autoregressive (LEAR) model serves as the univariate counterpart of CING-LEAR, providing a natural baseline to evaluate the value of multivariate cross-output learning and inclusion of group effects. It is presented in Section 3.2. More details can be found in [10].

### 4.2.6. DNN

The Deep Neural Network (DNN) benchmark, as proposed in [17], is a fully connected multi-layer perceptron (MLP) with a multi-output structure for jointly predicting the vector of day-ahead LMPs. The architecture consists of four layers: an input layer with the same inputs as in CING-LEAR, two hidden layers, and a linear output layer with 24 outputs representing each hourly LMP of the day. Each hidden layer is fully connected and employs the ReLU activation function. The output layer uses a linear activation to generate point forecasts. The implementation details and hyperparameter settings of LEAR and DNN follow the recommendations in [21].

### 4.2.7. Chronos-2

Chronos-2 is a pre-trained time series foundation model (TSFM) [32]. It leverages in-context learning and produces multi-step quantile forecasts. We include two variants of Chronos-2: A zero-shot version where the model is applied, as is, without in-context learning; and a fine-tuned version wherein we set the context length to 2048 (maximum setting) with a 24-hour prediction length.

### 4.3. Evaluation metrics

The following metrics for point and probabilistic forecast evaluation are used to evaluate CING-LEAR.

#### 4.3.1. Mean absolute error (MAE)

$$\text{MAE} = \frac{1}{24 \cdot N} \sum_{d=1}^N \sum_{h=1}^{24} |p_{d,h} - \hat{p}_{d,h}|,$$

where  $p_{d,h}$  denotes the observed electricity price at day  $d$  and hour  $h$ ,  $\hat{p}_{d,h}$  is the corresponding point forecast, and  $N$  is the number of days in the test set.

#### 4.3.2. Root mean squared error (RMSE)

$$\text{RMSE} = \sqrt{\frac{1}{24 \cdot N} \sum_{d=1}^N \sum_{h=1}^{24} (p_{d,h} - \hat{p}_{d,h})^2},$$

which penalizes large forecast errors more heavily due to the quadratic loss and thus provides complementary information to MAE regarding the dispersion of point forecast errors.

#### 4.3.3. Continuous ranked probability score (CRPS)

For a predictive distribution  $F_{d,h}(\cdot)$  and an observation  $p_{d,h}$ , the CRPS is defined as

$$\text{CRPS}(F_{d,h}, p_{d,h}) = \int_{-\infty}^{+\infty} (F_{d,h}(z) - \mathbb{1}\{z \geq p_{d,h}\})^2 dz,$$

where  $\mathbb{1}(\cdot)$  denotes the indicator function. In practice, CRPS is computed using a sample-based approximation. Given  $M$  Monte Carlo samples  $\{x_{d,h}^{(m)}\}_{m=1}^M$  drawn from the predictive distribution  $F_{d,h}$ , where  $M$  is chosen to be sufficiently large ( $M = 20,000$  in this study), CRPS can be expressed in its equivalent expectation form as:

$$\text{CRPS}(F_{d,h}, p_{d,h}) \approx \widehat{\text{CRPS}}(F_{d,h}, p_{d,h}) = \frac{1}{M} \sum_{m=1}^M |x_{d,h}^{(m)} - p_{d,h}| - \frac{1}{2M^2} \sum_{m=1}^M \sum_{m'=1}^M |x_{d,h}^{(m)} - x_{d,h}^{(m')}|.$$

The CRPS over the testing period is then computed as:

$$\text{CRPS} \approx \frac{1}{24 \cdot N} \sum_{d=1}^N \sum_{h=1}^{24} \widehat{\text{CRPS}}(F_{d,h}, p_{d,h}).$$

## 5. Result and Analysis

### 5.1. Forecasting Results

Figure 4 presents a representative period in April 2025, comparing the actual LMPs with the correspondent forecasts generated by LEAR, DNN, Chronos-2, and CING-LEAR. All four models appear to successfully capture the daily seasonality of LMPs, with lower prices during daytime hours and higher prices overnight, as well as two peaks around sunrise and sunset. For this representative period, all four models achieve relatively greater accuracy during night time. This may be caused by higher load and solar penetration during the day, which collectively induce greater variability into the LMPs. A noticeable visual distinction is how CING-LEAR produces smoother forecasts, which is due to the inclusion of group effects in the feature selection. This temporal smoothness enables CING-LEAR to be more consistent with actual LMP patterns, leading to improved accuracy and more realistic behavior (See, for example, the daytime hours in April 20).

Table 1 reports the average performance for 2024 and 2025, as well as the two-year average, across all methods considered. *Transform* refers to whether the data preprocessing steps described in Section 4.1 were applied. Please

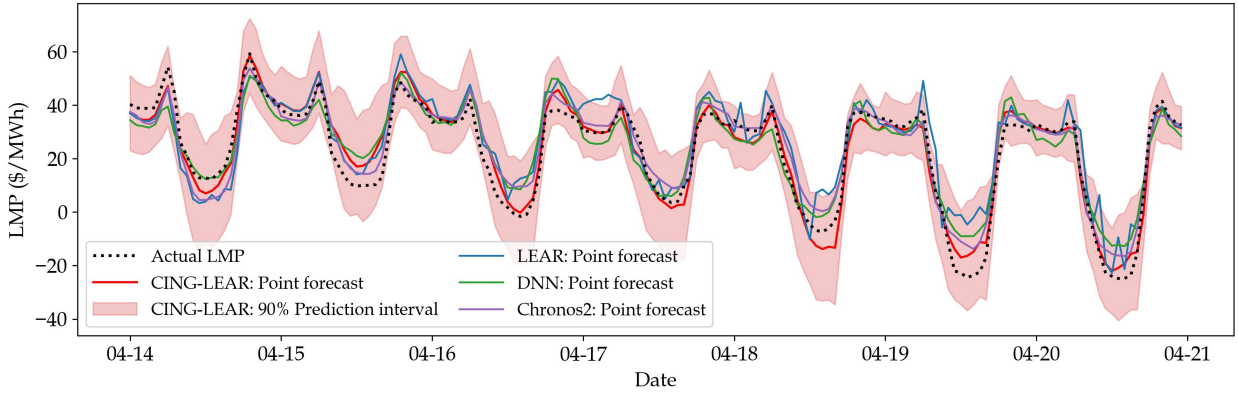


**Figure 4:** Comparison of actual LMPs and correspondent day-ahead forecasts over a representative period of one week in April 2025. The dashed line denotes the actual LMPs, while solid lines represent the forecasts produced by the different models (Red = CING-LEAR, Blue = LEAR, Green = DNN, Purple = Chronos-2). The red shaded region indicates the 90% prediction interval produced by CING-LEAR, showing faithful probabilistic coverage.

**Table 1**

Performance comparison among different forecasting models in terms of MAE, RMSE, and CRPS. Bold-faced and underlined values indicate the top and second-best performance, respectively.

	Method	MAE			RMSE			CRPS		
		2024	2025	Overall	2024	2025	Overall	2024	2025	Overall
Time Series Benchmarks	Naïve	10.670	9.734	10.203	20.593	14.433	17.786	8.077	6.635	7.356
	Seasonal Naïve	7.477	5.791	6.635	15.892	8.490	12.745	6.165	4.253	5.209
	ARIMA	10.650	9.626	10.139	20.702	14.193	17.753	8.092	6.611	7.352
	ARIMA (w/ transform)	10.546	9.607	10.077	27.882	28.494	28.188	8.017	6.581	7.299
	ARIMA-X	8.217	5.365	6.793	15.040	7.390	11.854	6.109	3.902	5.005
	ARIMA-X (w/ transform)	7.326	5.730	6.529	16.423	8.745	13.162	5.778	4.271	5.024
Advanced Methods	LEAR [10]	6.326	4.792	5.560	13.101	6.762	10.429	4.826	3.478	4.152
	DNN [17]	6.804	4.942	5.875	13.419	6.822	10.649	5.081	3.564	4.322
	Chronos-2 (zero-shot) [32]	6.080	4.172	5.128	14.171	5.829	10.840	5.054	3.053	4.053
	Chronos-2 (fine-tuned) [32]	5.823	3.984	4.905	13.980	5.595	10.653	4.891	2.920	3.905
Proposed	CING-LEAR	5.724	4.086	4.907	<b>11.342</b>	5.684	<b>8.974</b>	4.274	2.970	3.622
	CING-LEAR + Chronos-2	<b>5.362</b>	<b>3.809</b>	<b>4.587</b>	<u>11.639</u>	<b>5.335</b>	<u>9.057</u>	<b>4.182</b>	<b>2.783</b>	<b>3.482</b>

note that both LEAR and CING-LEAR use this transform as well. Looking at Table 1, few observations can be drawn. First, both LEAR and DNN clearly outperform the standard time series benchmarks—a conclusion that supports the potency of these methods for short-term EPF, as similarly demonstrated in prior studies [21]. Second, it appears that CING-LEAR consistently outperforms LEAR, DNN, and Chronos-2 (zero-shot), as well as all time series benchmarks, across all evaluation metrics. The performance of CING-LEAR is comparable to that of the fine-tuned Chronos-2, but with an important caveat. While both models produce comparable performance in 2025 across all metrics, the results of the year 2024 reveal an interesting insight: moderate improvement in MAE in favor of CING-LEAR (2%) but disproportionately significant improvements in both RMSE (19%) and CRPS (13%) in favor of CING-LEAR. If any, this suggests that CING-LEAR may be responding better to extreme and tail events, like price spikes and ramps, since the latter metrics place greater emphasis on such events compared to MAE. We do acknowledge that this conclusion warrants more in-depth analysis and sets the stage for potentially interesting combinations of these two fundamentally different techniques, and we leave this for future work.

The comparison between CING-LEAR and Chronos-2 reveals that statistical and TSFMs exhibit complementary strengths. As such, we consider a simple ensemble constructed as the mean of the predictions from CING-LEAR and Chronos-2 (fine-tuned). As shown in Table 1, the ensemble achieves a significantly better performance over its member constituents (CING-LEAR and Chronos-2), especially for MAE and CRPS, as well as against all competing

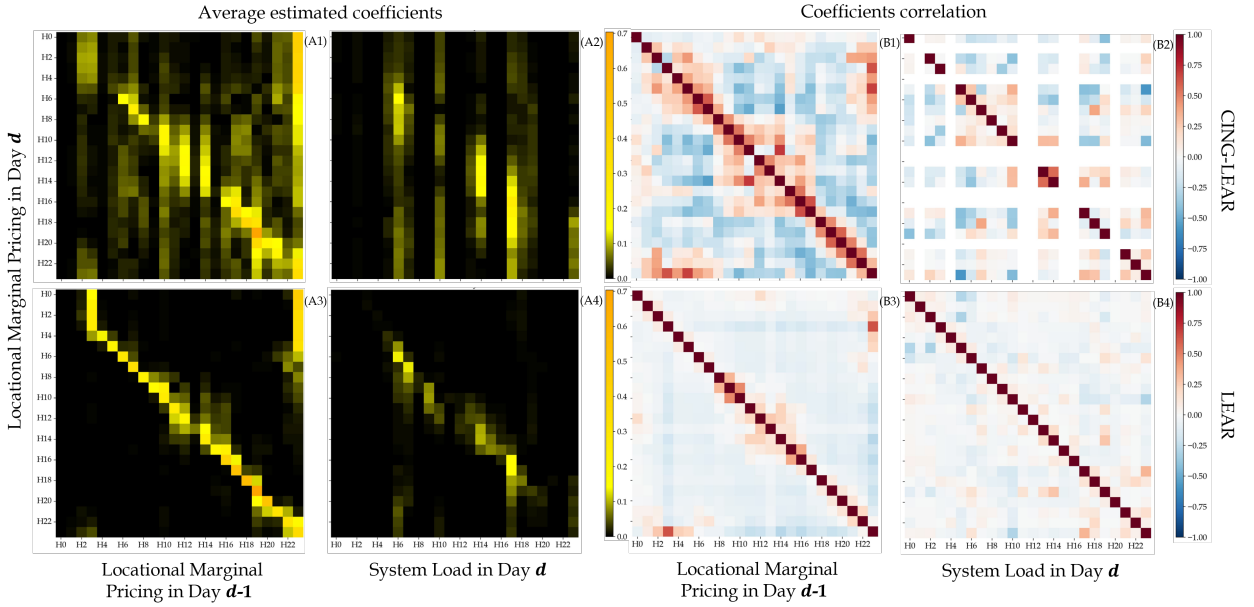


**Figure 5:** The left set of panels (A1-A4) display the estimated coefficients of each feature across the 24 hours, averaged over the entire test period, where black indicates zero coefficients and yellow colors correspond to absolute coefficient magnitudes. The right set of panel (B1-B4) show the correlation matrices of the coefficients across the 24 hourly, where red and blue denote positive and negative correlations, respectively. The first and second row corresponds to the CING-LEAR and the LEAR model, respectively. Due to page limitations, only two representative features are shown: the historical price in the previous day  $d - 1$  and the load forecast in the current day  $d$ .

benchmarks, suggesting that “the whole may be greater than the sum of its parts,” and that ensembles of rigorously crafted statistical models and fine-tuned TSFMs can be a fruitful path to pursue.

## 5.2. Feature Selection and Recovery

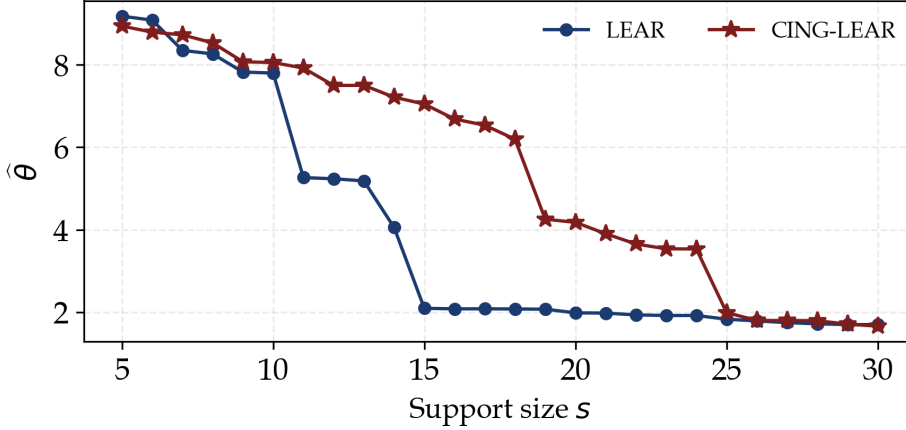
Figure 5(A) shows the estimated coefficients by LEAR (bottom row) which are largely concentrated around the diagonal, indicating that for each hourly LMP, only features associated with the same or nearby hours are retained. In contrast, CING-LEAR selects a broader set of features by capturing temporal group effects, aligning with the empirical analysis of pricing signals in Section 2. Interestingly, CING-LEAR also reinforces certain informative features already identified by LEAR. For instance, the LMP at the last hour in Day  $d - 1$  and the load at hours 14 and 17 show larger coefficient magnitudes under CING-LEAR than in LEAR.

Figure 5(B) shows the correlations among the estimated coefficients from CING-LEAR (top) and LEAR (bottom), wherein CING-LEAR exhibits more pronounced correlations among its coefficients across the day, indicating a stronger cross-hour structure in feature effects. Visually, the correlation matrix from CING-LEAR can be partitioned into three segments: hours 0- 7, 8-16, and 17-23. These segments appear to maintain highly positive in-segment correlations, and negative between-segment correlations. The relative smoothness of CING-LEAR’s forecasts (shown in Figure 4) can be explained in light of these pronounced correlations.

Another advantage of adopting a rigorous statistical approach like Group Lasso is our ability to leverage statistical regression theory to evaluate its performance, beyond predictive power. One such way is through a theoretical analysis of its ability to correctly recover underlying feature sets. Specifically, we define the support set associated with the group-sparse coefficient matrix as follows:

$$S = \{j \in \{1, \dots, M\} : \|\mathbf{b}_j\|_2 > 0\}.$$

which denotes the index set of selected feature groups in the coefficient matrix  $\mathbf{B}$ . We use  $S$  whenever referring to selected predictors in Figure 3. Under mild conditions [33], the feature selection performance can be governed by a



**Figure 6:** Estimated sample complexity parameter  $\hat{\theta}$  with respect to the support size  $s$  for LEAR and CING-LEAR.

sample complexity parameter:

$$\theta(N, M, \mathbf{B}) = \frac{N}{2\psi(\mathbf{B}) \log(M - s)}, \quad (16)$$

where  $s$  denotes the number of support features (non-zero). The term  $\psi(\mathbf{B})$ , referred to as the sparsity overlap function, depends on both the structure of  $\mathbf{B}$  and the covariance structure, and is defined as:

$$\psi(\mathbf{B}) = \left\| \mathbf{Z}_S^\top \boldsymbol{\Sigma}_{SS}^{-1} \mathbf{Z}_S \right\|_2, \quad (17)$$

where  $\mathbf{Z}_S$  denotes the normalized  $\mathbf{B}$  and  $\boldsymbol{\Sigma}_{SS}$  denotes the covariance submatrix, both restricted to the support  $S$ . Intuitively,  $\psi(\mathbf{B})$  quantifies the extent to which the active groups share common directions across tasks: smaller values correspond to stronger alignment and greater information sharing across outputs.

To compute  $\psi(\mathbf{B})$ , we use the estimated coefficient matrix  $\hat{\mathbf{B}}$ , and covariance matrix  $\hat{\boldsymbol{\Sigma}}$  as proxies for  $\mathbf{B}$  and  $\boldsymbol{\Sigma}$ , respectively. To approximate the true support  $S$ , we use an estimated support set  $\hat{S}$  constructed by selecting the  $s$  largest coefficients from  $\hat{\mathbf{B}}$ , to form a data-driven estimate  $\hat{\theta}$ , which serves as a diagnostic measure of the effective sample complexity relative to the degree of cross-task sparsity overlap present in the data. Figure 6 shows that  $\hat{\theta}$  decreases monotonically as the support size  $s$  increases. This behavior is consistent with the theoretical interpretation of  $\theta$ : enlarging the support set reduces the effective identifiability of the feature subspace and increases the difficulty of feature recovery. Two pronounced drops in  $\hat{\theta}$  are observed at support sizes 11 and 15 for LEAR, whereas the corresponding drops are delayed to 19 and 25 for CING-LEAR. In other words, for the same support size, CING-LEAR appears to maintain stronger feature recoverability than LEAR.

### 5.3. Benchmarking against the 2024 PG&E Energy Analytics competition

We further evaluate the performance of CING-LEAR by comparing it with the top performing teams in the 2024 PG&E Energy Analytics Challenge 2024 that focused on short-term EPF [5]. The training dataset consists of three years of hourly day-ahead LMPs for the NP15 region, from 2020 to 2022. A limited set of exogenous variables is provided, including regional load and natural gas prices. In addition to the provided information, the competition allowed participants to incorporate supplementary exogenous information into their forecasting models. The evaluation was carried out on a reserved test set that included LMPs from the first two weeks of 2023. During the forecasting stage, future day-ahead LMPs are excluded from the model inputs. Only historical exogenous information available up to the forecast time is permitted, ensuring a realistic day-ahead forecasting setting.

To ensure compliance by the competition rules, the day-ahead LMP forecasts for each day are used as inputs for subsequent daily forecasts throughout the two-week evaluation period. In Table 2, we compare the performance of CING-LEAR relative to the top three ranked teams from the challenge, along with the performance of statistical

**Table 2**

Performance comparison of CING-LEAR versus top-performing teams in the 2024 PG&E Energy Analytics Competition [5]. Bold-faced and underlined values indicate the top and second-best performance, respectively.

Method	# of added features	MAE	RMSE
Team 1 (LSTM with exogenous features)	46	<b>18.92</b>	<b>24.39</b>
Team 2 (Tree-based ensemble)	4	29.08	36.03
Team 3 (VAR + XGBoost)	1	26.82	35.17
Naïve	0	41.01	50.36
Seasonal Naïve (period = 24 hours)	0	38.00	46.30
ARIMA (no exogenous features)	0	38.40	48.10
ARIMA-X (w/ exogenous features)	0	32.30	44.00
LEAR [10]	0	27.78	36.49
CING-LEAR (Proposed)	0	<u>23.61</u>	<u>32.38</u>

**Table 3**

Forecasting performance comparison with industrial benchmarks. Bold-faced and underlined values indicate the top and second-best performance, respectively.

Method	7-month		12-month	
	MAE	RMSE	MAE	RMSE
Forecast_1	<b>4.95</b>	12.82	-	-
Forecast_2	5.84	<b>11.93</b>	<u>7.10</u>	<u>14.49</u>
CING-LEAR	<u>5.07</u>	<u>12.43</u>	<b>5.87</b>	<b>12.66</b>

benchmarks as reported by the challenge organizers [5]. The results show that Team 1 (an LSTM model with exogenous features) consistently outperforms all competing approaches across all evaluation metrics, benefiting from the use of a larger set of exogenous inputs (46 features). In contrast, without relying on additional features, CING-LEAR achieves second place among all participants. LEAR ranks a close third, further confirming its strength as a competitive model for short-term EPF.

#### 5.4. Benchmarking against industry operational models

CING-LEAR is independently validated against two models that are currently deployed by a major U.S. utility. Those are denoted as Forecast\_1 and Forecast\_2, respectively, and their technical details and identities are masked. Table 3 summarizes the forecasting performance of these two models and that of CING-LEAR over both 7-month (May to December 2024) and 12-month (January to December 2024) test periods. Over the 7-month period, where both industrial benchmarks are available, CING-LEAR achieves consistently competitive performance, ranking second in both MAE and RMSE (within 2-4% of the best-performing models), and is not dominated by any single competing approach. Over the full 12-month period, which provides a more comprehensive evaluation, CING-LEAR outperforms the available benchmark, achieving improvements of approximately 17% in MAE and 13% in RMSE. While the comparison set is more limited in this case, the results indicate strong and stable performance over an extended evaluation period. Overall, these findings demonstrate that CING-LEAR provides robust performance under strong competition and maintains high accuracy when evaluated over longer time spans, providing a strong indicator of industrial relevance, particularly given the maturity of such systems in practice.

## 6. Conclusion

This paper proposes CING-LEAR, a multivariate statistical method for short-term electricity price forecasting. Extensive, multi-year evaluations demonstrate that CING-LEAR delivers consistently strong forecasting performance relative to established benchmarks. In addition to improvements in point and probabilistic forecast quality, the resulting forecasts exhibit smooth temporal profiles, and interpretable signatures that reflect the model's ability to capture realistic cross-hour dependencies in electricity pricing signals.

This study also highlights several promising directions for future research. First, our study shows that combinations of diverse forecasters (e.g., CING LEAR with a TSFM) can indeed be promising. More advanced ensemble strategies

that exploit when and under which conditions do these models perform better can be proposed, for example based on performance, volatility, or regime indicators. Second, the proposed multivariate framework can be extended to jointly model electricity prices across multiple locations, enabling the explicit incorporation of spatial dependencies that are native to electricity pricing signals.

## Acknowledgment

This research is supported in part by the U.S. National Science Foundation, ECCS # 2114422.

## References

- [1] Lei Fan, Jianhui Wang, Ruiwei Jiang, and Yongpei Guan. Min-max regret bidding strategy for thermal generator considering price uncertainty. *IEEE Transactions on Power Systems*, 29(5):2169–2179, 2014.
- [2] Nicolo Mazzi, Jalal Kazempour, and Pierre Pinson. Price-taker offering strategy in electricity pay-as-bid markets. *IEEE Transactions on Power Systems*, 33(2):2175–2183, 2017.
- [3] Keyi Wang, Robert Mieth, and Ahmed Aziz Ezzat. From market signals to maintenance decisions: Grid-informed maintenance optimization in offshore wind farms. 2026.
- [4] Rafał Weron. Electricity price forecasting: A review of the state-of-the-art with a look into the future. *International Journal of Forecasting*, 30(4):1030–1081, 2014. doi: 10.1016/j.ijforecast.2014.08.008.
- [5] Ahmed Aziz Ezzat, Mahan Mansouri, Murat Yildirim, and Xiaolei Fang. IISE PG&E energy analytics challenge 2024: Forecasting day-ahead electricity prices. *IISE Transactions*, 58(1):117–129, 2026. doi: 10.1080/24725854.2024.2447049.
- [6] Antonio J Conejo, Javier Contreras, Rosa Espinola, and Miguel A Plazas. Forecasting electricity prices for a day-ahead pool-based electric energy market. *International Journal of Forecasting*, 21(3):435–462, 2005.
- [7] Hamidreza Zareipour, Claudio A Canizares, and Kankar Bhattacharya. Application of public-domain market information to forecast Ontario’s wholesale electricity prices. *IEEE Transactions on Power Systems*, 21(4):1707–1717, 2006.
- [8] Alberto Cruz, Antonio Muñoz, José Luis Zamora, and Rosa Espínola. The effect of wind generation and weekday on spanish electricity spot price forecasting. *Electric Power Systems Research*, 81(10):1924–1935, 2011.
- [9] Nektaria V Karakatsani and Derek W Bunn. Intra-day and regime-switching dynamics in electricity price formation. *Energy Economics*, 30(4):1776–1797, 2008.
- [10] Bartosz Uniejewski, Jakub Nowotarski, and Rafał Weron. Automated variable selection and shrinkage for day-ahead electricity price forecasting. *Energies*, 9(8):621, 2016.
- [11] Florian Ziel and Rafał Weron. Day-ahead electricity price forecasting with high-dimensional structures: Univariate vs. multivariate modeling frameworks. *Energy Economics*, 70:396–420, 2018.
- [12] Raffaele Sgarlato and Florian Ziel. The role of weather predictions in electricity price forecasting beyond the day-ahead horizon. *IEEE Transactions on Power Systems*, 38(3):2500–2511, 2023. doi: 10.1109/TPWRS.2022.3180119.
- [13] Jie Mei, Dawei He, Ronald Harley, Thomas Habetler, and Guodong Qu. A random forest method for real-time price forecasting in new york electricity market. In *2014 IEEE PES General Meeting | Conference & Exposition*, pages 1–5. IEEE, 2014.
- [14] Peng Wang, Bolun Liu, and Tianshu Hong. An online electricity market price forecasting method via random forest. *IEEE Transactions on Industry Applications*, 58(6):7013–7021, 2022.
- [15] Najeh Chaâbane. A novel auto-regressive fractionally integrated moving average–least-squares support vector machine model for electricity spot prices prediction. *Journal of Applied Statistics*, 41(3):635–651, 2014.
- [16] Xiaolong Xie, Wei Xu, and Hongzhi Tan. The day-ahead electricity price forecasting based on stacked CNN and LSTM. In *International Conference on Intelligent Science and Big Data Engineering*, pages 425–434. Springer, 2018.
- [17] Jesus Lago, Fjo De Ridder, and Bart De Schutter. Forecasting spot electricity prices: Deep learning approaches and empirical comparison of traditional algorithms. *Applied Energy*, 221:386–405, 2018.
- [18] Long Wang, Zijun Zhang, and Jieqiu Chen. Short-term electricity price forecasting with stacked denoising autoencoders. *IEEE Transactions on Power Systems*, 32(4):2673–2681, 2016.
- [19] Zhongxia Zhang and Meng Wu. Predicting real-time locational marginal prices: A GAN-based approach. *IEEE Transactions on Power Systems*, 37(2):1286–1296, 2021.
- [20] Zhongxia Zhang and Meng Wu. Real-time locational marginal price forecast: A decision transformer-based approach. In *2023 IEEE Power & Energy Society General Meeting (PESGM)*, pages 1–5. IEEE, 2023.
- [21] Jesus Lago, Grzegorz Marcjasz, Bart De Schutter, and Rafał Weron. Forecasting day-ahead electricity prices: A review of state-of-the-art algorithms, best practices and an open-access benchmark. *Applied Energy*, 293:116983, 2021.
- [22] Ronald Huisman, Christian Huurman, and Ronald Mahieu. Hourly electricity prices in day-ahead markets. *Energy Economics*, 29(2):240–248, 2007.
- [23] Anastasios Panagiotelis and Michael Smith. Bayesian density forecasting of intraday electricity prices using multivariate skew t distributions. *International Journal of Forecasting*, 24(4):710–727, 2008.
- [24] Niels Haldrup, Frank S Nielsen, and Morten Ørregaard Nielsen. A vector autoregressive model for electricity prices subject to long memory and regime switching. *Energy Economics*, 32(5):1044–1058, 2010.
- [25] Carolina García-Martos, Julio Rodríguez, and María Jesús Sánchez. Forecasting electricity prices by extracting dynamic common factors: Application to the Iberian market. *IET Generation, Transmission & Distribution*, 6(1):11–20, 2012.

- [26] Katarzyna Maciejowska and Rafał Weron. Forecasting of daily electricity prices with factor models: Utilizing intra-day and inter-zone relationships. *Computational Statistics*, 30(3):805–819, 2015.
- [27] Katarzyna Maciejowska and Rafał Weron. Short- and mid-term forecasting of baseload electricity prices in the uk: The impact of intra-day price relationships and market fundamentals. *IEEE Transactions on Power Systems*, 31(2):994–1005, 2016.
- [28] Gridstatus. URL <https://www.gridstatus.io/live/caiso>.
- [29] scikit-learn developers. `sklearn.linear-model.multitasklasso` — scikit-learn 1.4.0 documentation.
- [30] Han Liu, Mark Palatucci, and Jian Zhang. Blockwise coordinate descent procedures for the multi-task Lasso, with applications to neural semantic basis discovery. In *International Conference on Machine Learning*, 2009.
- [31] Bartosz Uniejewski, Rafał Weron, and Florian Ziel. Variance stabilizing transformations for electricity spot price forecasting. *IEEE Transactions on Power Systems*, 33(2):2219–2229, 2018. doi: 10.1109/TPWRS.2017.2734563.
- [32] Abdul Fatir Ansari, Oleksandr Shchur, Jaris Küken, Andreas Auer, Boran Han, Pedro Mercado, Syama Sundar Rangapuram, Huibin Shen, Lorenzo Stella, Xiyuan Zhang, Mononito Goswami, Shubham Kapoor, Danielle C. Maddix, Pablo Guerron, Tony Hu, Junming Yin, Nick Erickson, Prateek Mutalik Desai, Hao Wang, Huzefa Rangwala, George Karypis, Yuyang Wang, and Michael Bohlke-Schneider. Chronos-2: From univariate to universal forecasting. *arXiv preprint arXiv:2510.15821*, October 2025. doi: 10.48550/arXiv.2510.15821.
- [33] Guillaume Obozinski, Martin J. Wainwright, and Michael I. Jordan. Support union recovery in high-dimensional multivariate regression. *The Annals of Statistics*, 39(1):1–47, February 2011. doi: 10.1214/10-AOS793.